ELSEVIER

Journal of Structural Geology 30 (2008) 725–738

JOURNAL OF STRUCTURAL GEOLOGY

www.elsevier.com/locate/jsg

Differential displacement and rotation in thrust fronts: A magnetic, calcite twinning and palinspastic study of the Jones Valley thrust, Alabama, US Appalachians

James S. Hnat [a,*], Ben A. van der Pluijm [a], Rob Van der Voo [a], William A. Thomas [b]

[a] *Department of Geological Sciences, University of Michigan, Ann Arbor, MI 48109-1005, USA*
[b] *Department of Geological Sciences, University of Kentucky, Lexington, KY 40506-0053, USA*

Received 7 May 2007; received in revised form 23 January 2008; accepted 25 January 2008
Available online 13 February 2008

Abstract

To test whether a displacement gradient along a curved fault structure requires rotation, we studied the northeast-striking, northwest-verging, large-displacement Jones Valley thrust fault of the Appalachian thrust belt in Alabama. Paleomagnetism, anisotropy of magnetic susceptibility (AMS) and calcite twinning analysis, complemented by balanced cross-sections, were used to evaluate the presence and magnitude of any rotation. Remanence directions from the Silurian Red Mountain Formation reveal a prefolding magnetization acquired in the Pennsylvanian, whereas magnetic analysis shows a strong, bedding-parallel compaction fabric with a tectonic lineation. Paleomagnetic directions and magnetic lineations reveal no relative rotation between the hanging wall and footwall of the thrust fault. Rather than rotation, therefore, we interpret the Jones Valley thrust sheet as a structure that developed in a self-similar fashion, with lateral growth of the fault surface occurring coincident with growth into the foreland.

Keywords: Rotations; Southern Appalachians; Birmingham anticlinorium; Magnetic fabric; Paleomagnetism; Thrust kinematics; Jones Valley thrust; Red Mountain Formation

1. Introduction

Rotations have been recognized as common features in most foreland thrust belts (McCaig and McClelland, 1992; Allerton, 1998; Macedo and Marshak, 1999; Marshak, 2004; Weil and Sussman, 2004; Sussman et al., 2004). On the scale of individual thrust sheets, thrust displacement gradients along strike of a structure are often cited as the cause of that rotation (Bates, 1989; Allerton et al., 1993; Allerton, 1998; Bayona et al., 2003; Pueyo et al., 2004; Sussman et al., 2004; Soto et al., 2006; Oliva-Urcia and Pueyo, 2007), but this hypothesis has remained a topic of debate. Identifying rotations in thrust sheets is also important for understanding the three-dimensional development of thrust belts and has implications for evolution on the orogenic scale (i.e., oroclinal bending; Marshak, 2004; Weil and Sussman, 2004; Sussman et al., 2004). Along rotated thrust sheets, traditional methods of restoring balanced cross-sections underestimate the amount of true displacement, because plane strain conditions do not apply. Whether rotations predicted from variations in displacement along strike, as seen in a series of strike perpendicular balanced cross-sections, necessitate significant vertical-axis rotations has been tested only in a few cases. This provided the motivation for our integrated study of the Jones Valley thrust fault in the southern US Appalachians.

Rotations have been recognized in many thrust belts, especially through paleomagnetism (e.g., McCaig and McClelland,

* Corresponding author. Department of Geological Sciences, University of Michigan, 2534 CC Little Bldg, 1100 N University, Ann Arbor, MI 48109-1005, USA. Tel.: +1 734 764 1435; fax: +1 734 763 4690.
E-mail addresses: jhnat@umich.edu (J.S. Hnat), vdpluijm@umich.edu (B.A. van der Pluijm), voo@umich.edu (R. Van der Voo), geowat@uky.edu (W.A. Thomas).

0191-8141/$ - see front matter © 2008 Elsevier Ltd. All rights reserved.
doi:10.1016/j.jsg.2008.01.012

1992; Bayona et al., 2003; Sussman et al., 2004; Satolli et al., 2005), which has a resolution of about 10°, depending on the quality of the data (Weil and Sussman, 2004). Many of these investigations, however, focused on regional kinematics in areas where significant variation in strike of bedding, faults and fold axial surfaces is observed (Schwartz and Van der Voo, 1984; Weil et al., 2000, 2001; Speranza et al., 2003). Less common are studies that explore the role of rotations in the evolution of an individual thrust sheet, which often do not display a large variation in strike orientation between the hanging wall and footwall. In the Subbetic Zone of southern Spain, Allerton (1994) showed that 68° of rotation on an individual structure was accommodated by a change in thrust displacement of 8.5 km over 3.7 km along strike. While this example is perhaps extreme, the evolution of the Santo Domingo anticline, an 80 km long structure in the External Sierras of the Southern Pyrenees (Pueyo et al., 2002, 2004; Oliva-Urcia and Pueyo, 2007), may be a more common case. In that area, the thrust displacement gradient from a series of four balanced cross-sections predicts a clockwise rotation that is matched by the (~25°) rotation seen in paleomagnetic analysis.

Relative rotations can be identified via other methods other than paleomagnetism. Magnetic lineations determined from anisotropy of magnetic susceptibility (AMS) can also be used for identification of vertical-axis rotations (Somma, 2006; Cifelli et al., 2004). Additionally, a method not using magnetic properties for recognizing rotations involves paleostress orientations from analysis of calcite twins (e.g., Craddock et al., 1988; Kollmeier et al., 2000; Ong et al., 2007). Changes in the orientations of other pre-thrusting features such as cleavage, fractures and paleocurrent data can also be used (Nickelsen, 1979; Gray and Mitra, 1993; Apotria, 1995).

The Jones Valley thrust sheet in central Alabama (Figs. 1A,B) offers an excellent opportunity to study the role, if any, of rotation in the formation of a curved fault structure. On the basis of restoration of balanced cross-sections described in this paper, the Jones Valley thrust fault with the associated detachment fold from which it emerged, progressively increases in displacement along strike over ~80 km, where it is appears to decrease in

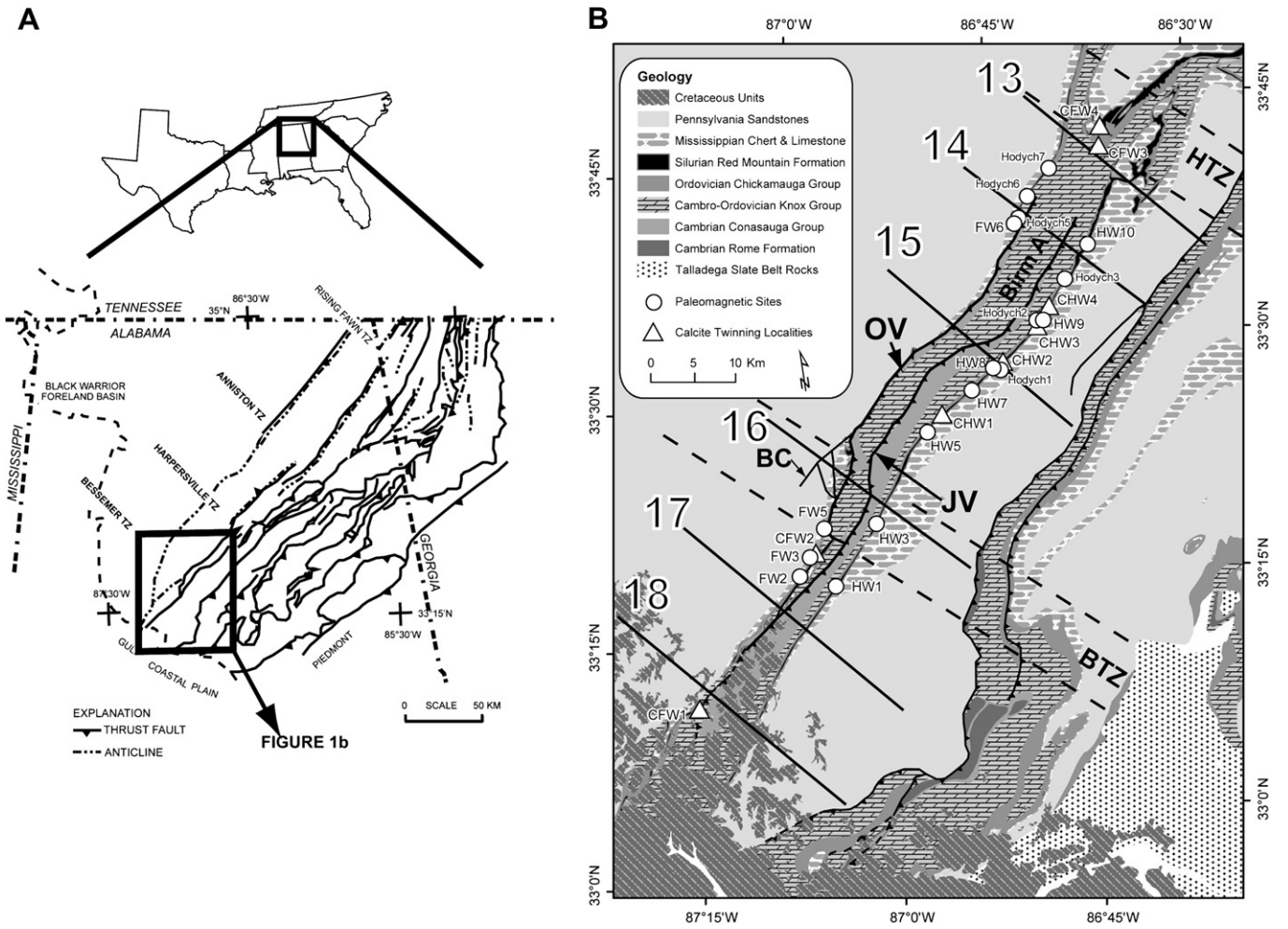

Fig. 1. (A) Map of Alleghanian thrust belt in Alabama and associated features (Redrawn from Thomas and Bayona, 2002). (B) Geologic map of study area based on Szabo et al. (1988). Lines labeled 13–18 represent cross-section lines of Fig. 2. OV – Opossum Valley thrust fault; JV – Jones Valley thrust; BC – Blue Creek fault; Birm A – Birmingham anticlinorium; HTZ – Harpersville transverse zone; BTZ – Bessemer transverse zone. Paleomagnetic (circles) from both this study and Hodych et al. (1985) and calcite twinning (triangles) sites are also shown.

displacement and is obscured by a cover of younger sediments to the southwest. A minimum rotation of 15° and upwards of 23° would be required to accommodate this displacement change. We considered this possibility by testing the hypothesis that the displacement gradient is the result of the self-similar evolution of the detachment fold and thrust rather than an artifact of rotation.

2. Structural setting

2.1. Appalachian foreland thrust belt

The study area lies within the Appalachian foreland thrust belt in Alabama (Fig. 1A) and is characterized by late Paleozoic (Alleghanian) deformation in the form of large scale, northeast-striking, generally northwest-verging thrust faults and associated folds (Rodgers, 1970; Hatcher et al., 1989; Thomas and Bayona, 2005). To the northwest, the belt is bounded by the Black Warrior foreland basin, consisting of late Paleozoic undeformed strata, and to the southeast, by the metamorphic thrust sheets of the Talladega slate belt and the Piedmont (Thomas and Bearce, 1986; Tull, 1998).

2.2. Jones Valley thrust fault

The large-displacement Jones Valley thrust fault and the associated Birmingham anticlinorium (Figs. 1B and 2) are in the southernmost exposed part of the Appalachian thrust belt. The Jones Valley thrust is a northeast-striking, northwest-verging thrust fault (Szabo et al., 1988) acting as the roof of a ductile duplex (defined as mushwad; Thomas, 2001; Thomas and Bayona, 2005), which consists of tectonically thickened Cambrian shales in the core of the Birmingham anticlinorium. The location of the Jones Valley thrust ramp is dictated by a down-to-the-southwest basement normal fault beneath the allochthon. Ahead of the Jones Valley thrust, within the anticlinorium, the Opossum Valley thrust fault (Figs. 1B and 2a), a footwall splay, parallels the Jones Valley thrust; however, at the Bessemer transverse zone, the Opossum Valley thrust sheet ends abruptly at a lateral ramp. The footwall of the Jones Valley/Opossum Valley thrust system within the forelimb of the Birmingham anticlinorium is continuous and steeply dipping to overturned to the northwest, whereas the hanging wall is gently dipping to the southeast and forms the trailing limb of the anticlinorium. The asymmetry of the anticlinorium and presence of the Palmerdale/Bessemer ductile duplex defines the Birmingham anticlinorium as a complex detachment fold offset by the Jones Valley/Opossum Valley thrust system (Thomas, 2001; Thomas and Bayona, 2005). Little difference exists between the strike of bedding in the footwall and hanging wall along the length of the fault except for a minor variation at the position of the Bessemer transverse zone. Bayona et al. (2003) interpreted rotations, using changes in local strike orientations at lateral ramps, as well as thrust displacement gradients in transverse zones to the northeast of the study area. However, similar to the work of Allerton (1994), the lack of significant variation in map-view strike orientation between hanging wall and footwall of the Jones Valley thrust gives no information as to the presence or amount of rotation.

In the northeast, the Jones Valley thrust sheet emerges from a small anticline in the crest of the Birmingham anticlinorium. The appearance of the Jones Valley thrust fault in the northeast is along the alignment of the cross-strike links in the Harpersville transverse zone. Along strike to the southwest, the Jones Valley thrust fault crosses the Bessemer transverse zone, where a lateral ramp accommodates displacement at the end of the leading Opossum Valley thrust fault. Farther to the southwest, other than the small displacement Blue Creek fault and a very minor backthrust, the Jones Valley thrust fault is the only structure accommodating shortening within the anticlinorium. At the southwest end of the study area, the Jones Valley thrust fault and associated Birmingham anticlinorium are covered by Cretaceous coastal plain sediments.

2.3. Displacement along the Jones Valley thrust fault

A series of previously published cross-sections in the Appalachian thrust belt of Alabama allow comparison of displacement magnitudes along strike for the Jones Valley thrust fault (Fig. 2) (Thomas and Bayona, 2005). The cross-sections were constructed perpendicular to thrust belt strike and based on seismic profiles, outcrop data and wells. Palinspastic restoration was completed using a combination of bed-length and area-balancing techniques (e.g. Dahlstrom, 1969; Marshak and Mitra, 1988).

While displacement estimates in the southern Appalachians are not as well constrained as those in other, younger thrust belts (e.g., Pyrenees, Wyoming-Idaho, Taiwan belts) due to the lack of preserved hanging wall cutoffs, the series of cross-sections (Fig. 2; Thomas and Bayona, 2005) provides estimates of minimum displacement on the Jones Valley thrust fault (Table 1). A comparison of the palinspastically restored cross-sections of the Jones Valley thrust sheet shows a displacement increase of greater than 20 km from the northeast termination (cross-section 13 and 14) to the southwest (cross-section 17 and 18). Thrust displacement on is near zero at the northeast termination (cross-section 13 and 14), where regional shortening is largely accommodated by folding in the Birmingham anticlinorium. Displacement increases to more than 20 km farther southwest (cross-section 17) and appears to decrease slightly farther to the southwest (cross-section 18). A minimum vertical-axis rotation of approximately 15° could produce this strike-parallel displacement gradient. This estimate is a minimum:

1) Rotation would entail out-of-plane motion of the thrust sheet, thereby underestimating displacement values from the strike-perpendicular cross-sections.
2) Hangingwall cutoffs are not preserved and displacement estimates are at a minimum in the southwestern section (cross-section 17). However, estimates are not a minimum in the northeastern section (cross-section 13 and 14) where much of the shortening is taken up in the folding of the Birmingham anticlinorium (Table 1). This situation would, therefore allow a greater angle of rotation.

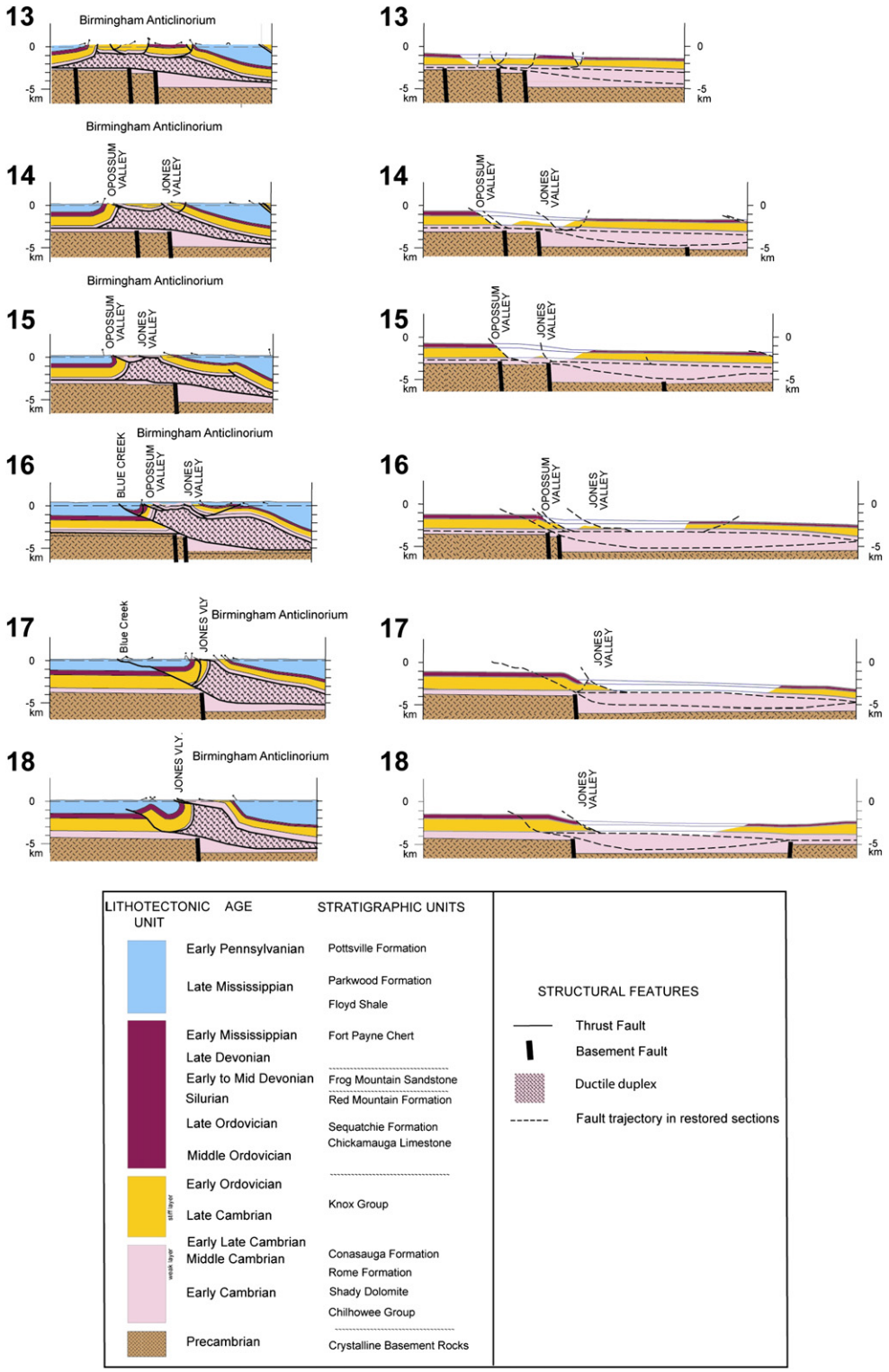

Fig. 2. Cross-section lines (modified from Thomas and Bayona, 2005) used to determine displacement variation. The Jones Valley thrust sheet terminates between cross-sections 13 and 14 and increases in displacement to the southwest in cross-sections 17 and 18.

3) Thermal data from vitrinite reflectance of Pennsylvanian coals suggest a high temperature anomaly in the eroded footwall of the Jones Valley thrust sheet (Winston, 1990; O'Hara et al., 2006). Assuming that the thermal anomaly results from a greater cover dues to additional tectonic burial by the Jones Valley thrust sheet, greater displacement and hence rotation magnitude would be expected.

While the lower limit of the postulated rotation is near the resolution limit for paleomagnetism ($\sim 10^{\circ}$), the high quality

Table 1
Table presenting displacement data derived from cross-sections and length from tip data derived from the map

Cross-section	Distance from tip (km)	Displacement (km)
14	4.8	2.0
15	20.9	5.0
16	42.4	14.0
17	59.9	21.0
18	73.2	16.0

Displacements are minima, as hanging wall cutoffs are not preserved in the Appalachians.

of the paleomagnetic data from this study allows for the determination of role of vertical-axis rotations in the evolution of the Jones Valley thrust sheet.

Assuming negligible internal shortening, which is typical of foreland thrust sheets of the southern Appalachians (House and Gray, 1982; Hatcher et al., 1989), one interpretation of the displacement geometry of the thrust sheet involves a vertical-axis rotation of 15°–23° of the Jones Valley thrust sheet toward the foreland, whereas an alternative scenario simply involves differential translation on the thrust (Fig. 3). The rotation model has a fixed hinge point and treats the thrust sheet as a rigid body. Conversely, the differential translation model requires that there is no fixed hinge and that the thrust grew laterally while displacing toward the foreland. This self-similar style growth (Elliott, 1976; Fischer and Woodward, 1992) would require internal deformation of the thrust sheet in the form of minor shear strain, with implications for the continuity of the thrust sheet (Wilkerson, 1992).

The relatively straight frontal ramp of the Jones Valley thrust fault, the large displacement gradient from northeast to southwest and the presence of suitable rock types allows for a relatively simple test of the role of vertical-axis rotation for the evolution of the Jones Valley thrust sheet. To investigate both the occurrence and amount of rotation, we employ paleomagnetic and anisotropy of magnetic susceptibility (AMS) analysis of the Silurian Red Mountain Formation, as well as calcite twinning of the underlying Chickamauga Group limestones.

3. Unit description

The stratigraphy of the study area is the regionally characteristic succession in most of the southern Appalachians (e.g. Butts, 1926; Chowns and McKinney, 1980; Thomas, 1977). Lower to Middle Cambrian sediments (Chilhowee Group, Shady Dolomite, Rome Formation and Conasauga Formation) associated with Iapetan rifting overlie faulted Precambrian basement and represent the regional basal detachment level (Thomas, 1991). Mudstones and limestones of the Middle Cambrian Conasauga Formation form the oldest exposed rocks and represent the major ductile unit involved in duplex development. The Cambro-Ordovician Knox Group dolomites and limestones form the regional stiff layer contained in thrust sheets (Thomas and Bayona, 2005).

Unconformably overlying the Knox Group are limestones of the Middle to Upper Ordovician Chickamauga Group. The Chickamauga Group consists of a range of limestone units, including calcareous mudstones, peloidal grainstones and fossiliferous grainstones (Rindsberg and Osborne, 2001; Rindsberg et al., 2003). For calcite twinning analysis, emphasis was placed on sampling the coarser grainstones.

The Red Mountain Formation is a heterogeneous clastic unit that comprises the entire package of Silurian stratigraphy within the thrust belt in Alabama (Chowns and McKinney, 1980). It unconformably overlies the Chickamauga Group limestones. Biostratigraphic studies indicate that the unit ranges from Early Silurian (Llandoverian) age (Berry and Boucot, 1970) to Late Silurian (Pridolian) age (Berdan et al., 1986) with various internal disconformities (Rindsberg et al., 2003). The lithology of the Red Mountain Formation includes massive and laminated reddish hematitic sandstones, oolitic ironstones, interbedded shales and gray sandstone, lesser pebble conglomerate beds and some minor limestone lenses. Sampling of the Red Mountain Formation focused on

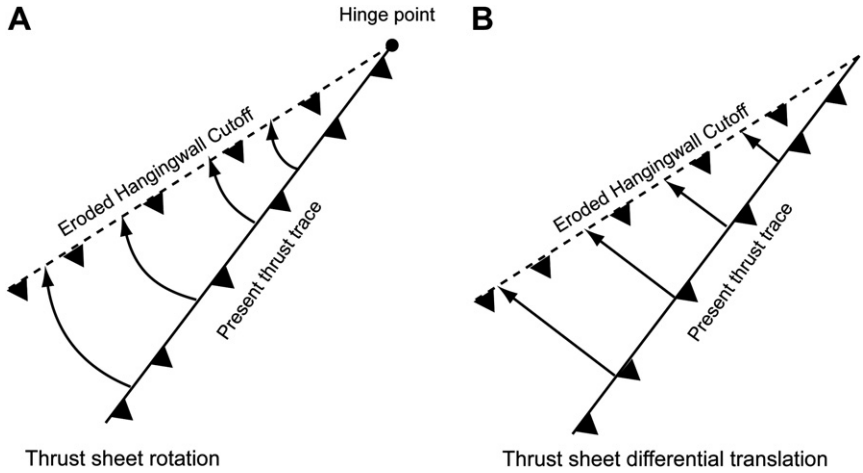

Fig. 3. Schematic illustration showing two scenarios for the development of a thrust sheet with the same displacement gradient. In (A), the thrust sheet rotates to its final position. In (B), the thrust sheet displaces differentially along strike.

the hematitic sandstones and ironstones best suited for paleomagnetic analysis. In the study region, the Red Mountain Formation is unconformably overlain by the Devonian Chattanooga Shale, Mississippian Maury Shale or the Mississippian Fort Payne Chert, although thin units of the Devonian (Frog Mountain Formation) are present in some locations. The youngest units involved in the deformation are Pennsylvanian clastic deposits.

4. Paleomagnetism and magnetic susceptibility

4.1. Methods

Samples were collected from eleven sites in the Red Mountain Formation along the strike of the Jones Valley thrust sheet. Sampling focused on red sandstones and ironstones that had been successfully analyzed in past studies of the formation (Perroud and Van der Voo, 1984; Hodych et al., 1985). Four sites are located on the northwest-dipping to overturned footwall and seven sites on the southeast-dipping hanging wall (Fig. 1B). Site selection was controlled by both limited outcrop availability in this area due to the high degree of weathering, and position along strike with respect to the Jones Valley thrust fault. Between seven and twelve 2.5 cm diameter samples were collected at each site using a portable gasoline powered drill, so 106 total samples were collected. Bedding attitude and core orientations were measured using a magnetic compass. Prior to analysis, the samples were cut into 2.5×2.2 cm cylindrical specimens at the University of Michigan's Paleomagnetic Laboratory for paleomagnetic and anisotropy of magnetic susceptibility (AMS) work.

All 2.5×2.2 cm specimens of the Red Mountain Formation were first measured for anisotropy of magnetic susceptibility (AMS). Specimens were measured in the fifteen-position method of Jelinek (1978) on a Geofyzika Brno Kappabridge KLY-2.03 susceptibility-bridge at a frequency of 920 Hz (coil sensitivity is approximately 5×10^{-7} SI). Analysis was performed using linear perturbation analysis producing a statistical bootstrap of the data using the 'bootams' program of Tauxe (1998). Bootstrap eigenvectors are plotted and displayed as a smear of points on a stereonet (e.g., Pares and van der Pluijm, 2002a). To infer relative contributions of ferromagnetic (generally magnetite and hematite) and paramagnetic (commonly phyllosilicate) grains to the susceptibility, bulk susceptibility was measured both at room temperature ($\sim$290K) and at the temperature of liquid nitrogen (77K). Bulk susceptibility of ferromagnetic grains does not change at low temperature while that of paramagnetic grains increases $\sim$3.8 times at 77K according to the Curie–Weiss law (Richter and van der Pluijm, 1994; Pares and van der Pluijm, 2002b).

Thermal demagnetization was carried out on all samples within a magnetically shielded, low-field room using an Analytical Service Co. (ASC) thermal demagnetizer. Samples were measured in a three-axis, cryogenic 2G Enterprises Model 755 Superconducting magnetometer after each heating step, with stepwise demagnetization ranging from 100 °C and 680 °C. Demagnetization was discontinued when the sample intensity approached zero percent of the natural remanent magnetization (NRM) or became erratic because of spurious magnetizations acquired during the cooling process.

Principal component analysis (Kirschvink, 1980) of linear vectors selected from orthogonal projection demagnetization plots (Zijderveld, 1967) was used to calculate the characteristic remanent magnetization (ChRM) with the SuperIAPD software package (Torsvik et al., 1999). Individual sample ChRM directions were used to determine site means using Fisher's

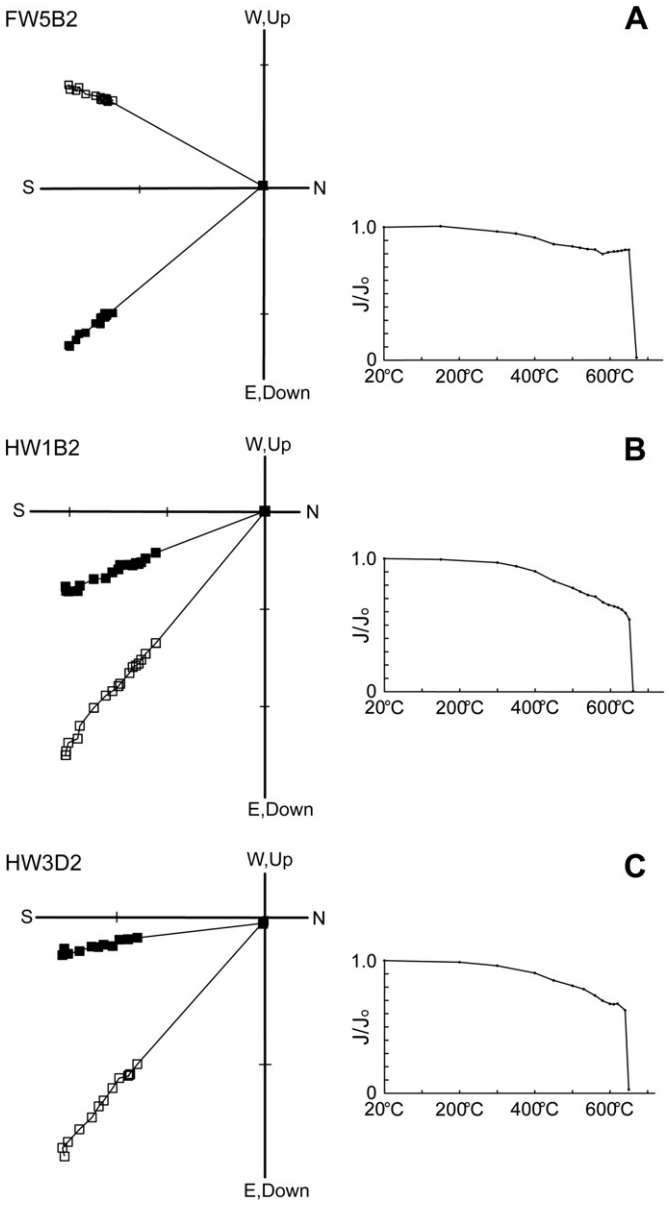

Fig. 4. Representative thermal demagnetization plots of the Red Mountain Formation in geographic coordinates and associated intensity plots. Intensity plots show normalized intensity versus temperature in degrees Celsius. In the demagnetization plots, closed (open) symbols represent vector endpoints plotted in the horizontal (vertical) plane. Temperature steps are in degrees Celsius. (A) Representative footwall sample showing the southeast and up direction. (B, C) Representative hanging wall samples showing southeast and down direction. Sharp decreases in intensity occur near 640 °C in most samples. Ticks represent 50 mA/m.

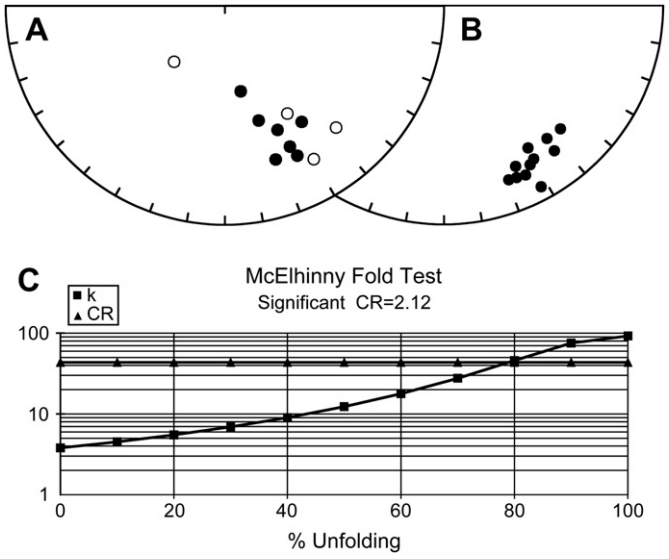

Fig. 5. (A, B) Equal area projections of site means in geographic (A) and tilt-corrected (B) coordinates. Solid (open) circles represent down (up) directions. (C) Incremental fold test of site means plotting k on logarithmic scale versus percent unfolding. Squares represent k values and triangles represent the critical ratio (CR) at which k values become significant at the 95% confidence level for the number of data entries (McElhinny, 1964).

(1953) method. The age of magnetization relative to deformation was tested using a fold-test on the site mean directions (McElhinny, 1964).

4.2. Paleomagnetic results

Intensities of the NRM for the Red Mountain Formation vary between 10 and 220 mA/m. Stepwise thermal demagnetization typically reveals univectorial decay of a single magnetic component (Fig. 4). Heating steps began at 100 °C intervals up to 400 °C and then were decreased progressively during heating until 10 °C intervals were used above 620 °C. In general, specimen intensity tends to remain stable up to a range from 640 °C to 680 °C, where intensity drops suddenly to <20% of the NRM. This high laboratory unblocking temperature (T_{lab}) indicates that hematite is the carrier of the magnetization, as expected.

In situ, site mean directions for the seven hanging wall sites reveal an intermediate down and southeast direction in all sites (Figs. 4 and 5) while in situ footwall site mean directions display intermediate up and southeast directions except for site FW2, which has a steeply up and southwest direction. After tilt correction, the site means cluster in a southeast down direction of $D = 150.4°$, $I = 18.5°$, $\alpha 95 = 4.8°$ and $k = 92.29$ (Table 2). This direction for the Red Mountain

Table 2
Paleomagnetic results from the Red Mountain Formation

	Latitude	Longitude	Strike	Dip	N/N_o	Dec In situ	Inc In situ	Dec Tilt	Inc Tilt	$\alpha 95$	k
Footwall											
FW2	33.304°N	87.076°W	218°	110°	7/7	222.2°	−61.8°	157.3°	15.6°	14.9°	17.27
FW3	33.323°N	87.057°W	238°	40°	8/9	149.9°	−20.2°	149.9°	19.8°	5.3°	110.31
FW5	33.352°N	87.037°W	193°	58°	10/10	137.6°	−25.7°	136.9°	23.5°	7.2°	45.53
FW6	33.646°N	86.743°W	190°	75°	7/9	149.9°	−42.6°	142.5°	24.1°	6.3°	92.69
Mean	–	–	–	–	4/4	–	–	146.8°	20.9°	10.5°	77.88
Hodych5	33.645°N	86.743°W	185°	73°	8	145.5°	−33.5°	138.3°	20.2°	4.5°	153
Hodych6	33.657°N	86.738°W	207°	52°	9	149.6°	−18.9°	151.3°	25.4°	9.4°	31
Hodych7	33.678°N	86.717°W	214°	41°	8	153.6°	−15.8°	154.4°	20.1°	6.3°	77
Mean with Hodych sites	–	–	–	–	7/7	–	–	147.3°	21.4°	6.1°	97.96
Hangingwall											
HW1	33.290°N	87.032°W	35°	38°	12/12	169.5°	57.4°	149.7°	25.3°	5.2°	70.04
HW3	33.349°N	86.970°W	32°	34°	9/9	163.6°	44.6°	151.8°	18.3°	7.6°	46.69
HW5	33.437°N	86.890°W	42°	20°	11/12	154.2°	25.0°	152.0°	6.6°	6.1°	57.23
HW7	33.474°N	86.826°W	35°	20°	9/9	146.5°	36.6°	143.0°	17.7°	4.4°	140.66
HW8	33.496°N	86.789°W	62°	18°	9/9	157.0°	38.4°	156.2°	20.5°	5.7°	81.15
HW9	33.536°N	86.725°W	58°	15°	11/11	155.2°	29.9°	154.5°	15.0°	5.0°	83.53
HW10	33.610°N	86.654°W	47°	12°	9/9	161.7°	27.0°	159.8°	16.0°	5.7°	83.24
Mean	–	–	–	–	7/7	–	–	152.4	17.1°	5.7°	112.5
Hodych1a	33.495°N	86.788°W	57°	20°	5	150.9°	40.3°	150.2°	20.3°	2.5°	929
Hodych1c	33.495°N	86.788°W	54°	21°	3	150°	37.1°	149°	16.2°	3.4°	1284
Hodych1d	33.495°N	86.788°W	54°	21°	11	152°	37.9°	150.6°	17.1°	3.7°	156
Hodych1e	33.495°N	86.788°W	54°	21°	3	146°	37.1°	145.7°	16.1°	6.2°	396
Hodych1f	33.495°N	86.788°W	45°	20°	3	155.1°	37.5°	151.7°	18.5°	9.5°	171
Hodych2	33.537°N	86.723°W	34°	13°	6	158°	24°	155.6°	13.1°	9°	57
Hodych3	33.560°N	86.707°W	40°	16°	4	152.5°	37.1°	149.2°	22.1°	10.1°	84
Mean with Hodych sites	–	–	–	–	14/14	–	–	151.4°	17.4°	3.0°	181.98
Overall mean	–	–	–	–	11/11	–	–	150.4°	18.5°	4.8°	92.29
Overall mean with Hodych sites	–	–	–	–	21/21	–	–	150.2°	19.0°	3.5°	107.74

Mean directions are calculated from site means (Fisher, 1953); N/N_o, number of samples (sites) accepted/studied; Dec, declination; Inc, inclination; $\alpha 95$, radius of confidence circle in degrees; k, precision parameter (Fisher, 1953). Means calculated with and without sites from Hodych et al. (1985). Site FW2 dip is 110°, indicating overturned bedding.

Formation agrees with those of two previous studies by Perroud and Van der Voo (1984) and Hodych et al. (1985).

4.3. Relative timing of magnetization

To obtain the timing of acquisition of the magnetization, a fold test was carried out on all site means. Progressive unfolding of the site mean directions indicates that the magnetization was acquired prior to tectonic tilt; the precision parameter k increases from 3.8 at 0% unfolding to 92.3 at 100% unfolding (Fig. 5). Because the footwall sites lie on the steeply dipping forelimb and the hanging wall sites are in the gently dipping trailing limb of the Birmingham anticlinorium, a 100% positive fold test implies that the magnetization was acquired prior to formation of the anticlinorium. Therefore, because the Jones Valley thrust fault and its frontal imbricate, the Opossum Valley thrust fault, are intimately related to the formation of the Birmingham anticlinorium, the magnetization was acquired prior to motion on the Jones Valley thrust fault.

Although the magnetization is clearly pre-deformation (Fig. 5), a conglomerate test by Perroud and Van der Voo (1984) showed a well clustered ($k \approx 170$), non-random distribution of directions from pebbles from a conglomerate layer, with a tectonically corrected mean direction similar to the other sites. This implies a post-depositional, remagnetized direction for the Red Mountain Formation. Comparison of our calculated paleopole position (38°N 130°E) with the Laurentian apparent polar wander path (APWP: Van der Voo, 1993)

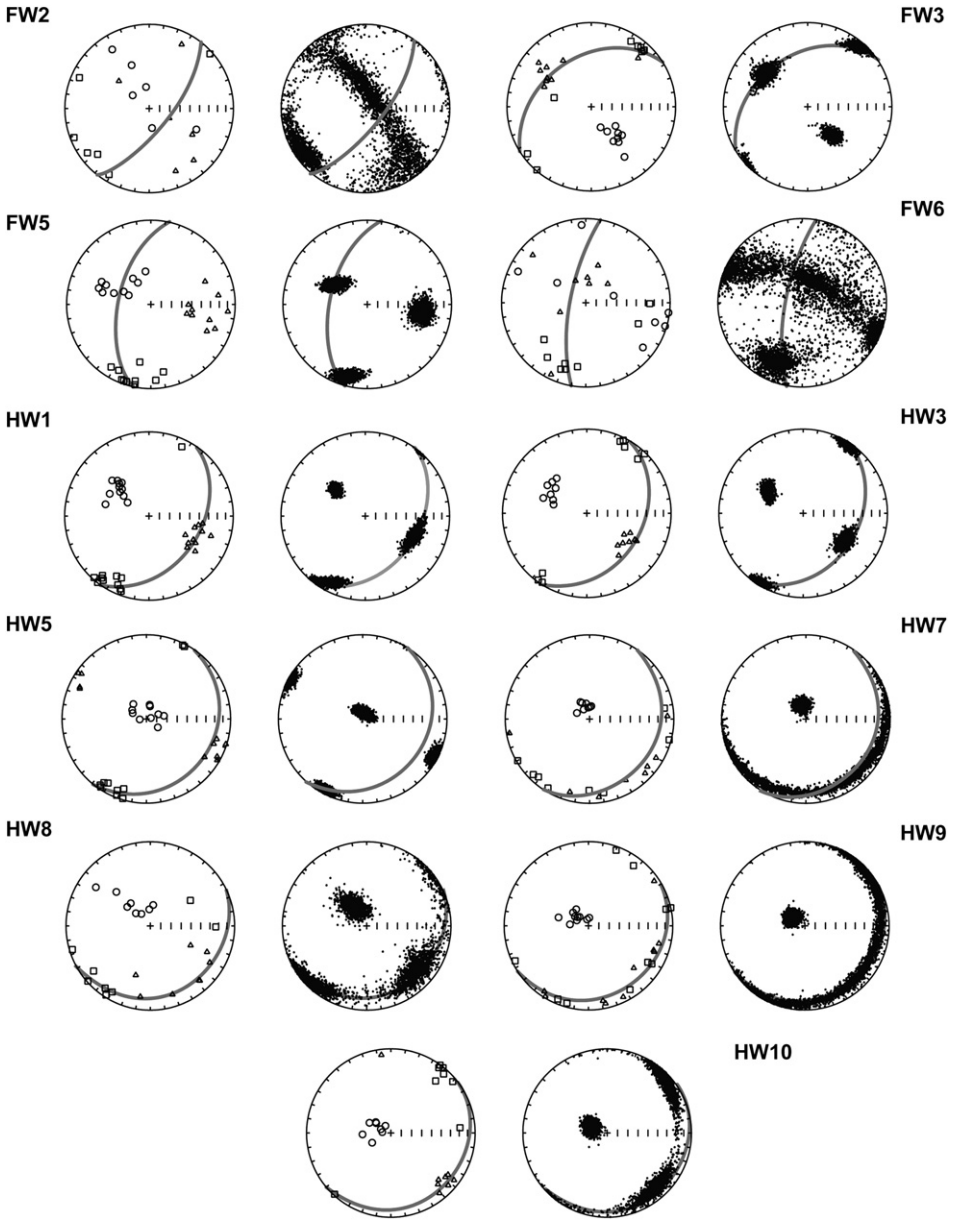

Fig. 6. Lower hemisphere, equal area projections showing AMS tensor properties for each site. Left stereoplot for each site shows calculated sample eigenvectors, with squares representing K_{max}, triangles representing K_{int} and circles representing K_{min}. The right projection is the bootstrapped eigenvectors derived from the data on the left showing a smear of points that better illustrates the tectonic lineation. All projections are in tilt-corrected coordinates.

indicates that the Red Mountain Formation acquired a remanence by chemical remagnetization during the Pennsylvanian, which is in agreement with the conclusions of previous workers (Perroud and Van der Voo, 1984; Hodych et al., 1985).

4.4. AMS results

Anisotropy of Magnetic Susceptibility (AMS) of the Red Mountain Formation reveals a compaction foliation in most sites, as indicated by perpendicular orientation of the minimum susceptibility axes (K_{min}) to the bedding plane (Fig. 6); most AMS ellipsoids display a triaxial shape (Table 3). This foliation is typically strong and dominates most samples, as indicated by the Flinn diagram (Fig. 7A). However, in the footwall, site FW2 shows a spread of K_{min} from horizontal to vertical, creating a swath in the bootstrap eigenvector plot (Fig. 6). Also, site FW5 displays a K_{min} that is bedding-parallel and orthogonal to the trace of the Jones Valley thrust fault. This effect occurs during layer-parallel shortening (LPS) that may be expected on the footwall/leading limb of a fault-related fold (Saint-Bezar et al., 2002).

At many sites, the maximum susceptibility axes (K_{max}) are oriented in a dominantly NE-SW orientation that is approximately parallel to the trace of the Jones Valley thrust fault. This intersection lineation is well defined in all footwall sites. On the hanging wall, it is well developed to the southwest at HW1, HW3 and HW5, as well as HW8. The tectonic lineation is less apparent in HW7, HW9 and HW10, where the AMS ellipsoid represents a purely compaction fabric. While all site means from the hanging wall lie in the oblate realm of the Flinn diagram (Fig. 7A), some footwall site means lie in the prolate domain of the plot, once again indicating greater amounts of LPS in the footwall.

Comparison of the bulk susceptibility at low temperature (~77K) and at room temperature (~290K) reveals a ratio of 1.1 (Fig. 7B). The lack of variation between low temperature and room temperature bulk susceptibilities indicates that the susceptibility is dominated by ferromagnetic grains. As previously mentioned, the high T_{lab} and sharp drop in intensity during thermal demagnetization signify hematite as the dominant ferromagnetic component. Therefore, the susceptibility is inferred to be dominantly carried by hematite.

5. Calcite twinning

5.1. Methods

Both oriented hand samples and standard paleomagnetic cores of fossiliferous limestones of the Middle to Upper Ordovician Chickamauga Group were collected from two sites on the steep to overturned footwall (Sites CFW1–2), two sites to the northeast of the termination of the Jones Valley thrust fault (Sites CFW3–4), and four sites from the hanging wall (Sites CHW1–4) of the Jones Valley thrust sheet for paleostress/strain analysis using calcite twin analysis (Fig. 1B). Since the formation of calcite twins is a strain hardening process (Teufel, 1980), twinning patterns commonly preserve bedding-parallel shortening, recording the earliest deformation (e.g. Groshong, 1972, 1974; Engelder, 1979; Spang and Groshong, 1981), and therefore act as a passive marker to record rotation (Craddock et al., 1988; Kollmeier et al., 2000; Ong et al., 2007). Because of the limited number of suitable samples that could be analyzed, limestone samples were cut into three mutually perpendicular thin sections to maximize data acquisition and were measured on a Zeiss Universal Stage (U-Stage) microscope. Only straight, continuous twinsets were measured to ensure the most accurate results. The measurements generally followed the procedure in Evans and Groshong (1994). After rotating thin sections into a common coordinate system, compression axes were calculated for each twinset using the method of Turner (1953) and mean paleostress orientations were determined using dynamic analysis of the compression axes (Spang, 1972). Strain tensor determinations using Groshong's (1972, 1974) method were calculated to separate positive and negative expected values in order to "clean" the data and identify multiple deformations (Teufel, 1980; Groshong et al., 1984). All twinning

Table 3
Anisotropy of Magnetic Susceptibility (AMS) results from the Red Mountain Formation

	Strike	Dip	N	τ_1	τ_1 T/P	τ_2	τ_2 T/P	τ_3	τ_3 T/P	χ_m	L	F	P	T
Footwall														
FW2	218°	110°	7	0.33629	48.4°/15.5°	0.33240	244.1°/74.0°	0.33131	139.5°/4.1°	144.42	1.014	1.005	1.020	0.471
FW3	238°	40°	9	0.33839	222.6°/5.8°	0.33415	312.8°/1.5°	0.32746	57.0°/84.0°	508.46	1.014	1.021	1.035	0.104
FW5	193°	58°	10	0.33725	203.1°/11.7°	0.33363	61.6°/75.1°	0.32912	295.0°/9.0°	252.14	1.012	1.016	1.027	0.140
FW6	190°	75°	9	0.33522	202.0°/22.9°	0.33318	42.7°/65.7°	0.33160	295.3°/7.7°	350.93	1.009	1.008	1.016	0.160
Hangingwall														
HW1	35°	38°	12	0.33590	209.8°/9.1°	0.33432	112.7°/37.7°	0.32978	311.2°/50.8°	371.06	1.005	1.015	1.019	0.445
HW3	32°	34°	9	0.33658	34.5°/3.1°	0.33390	127.1°/40.1°	0.32951	300.8°/49.8°	664.96	1.009	1.014	1.023	0.241
HW5	42°	20°	12	0.33761	206.6°/5.3°	0.33363	116.3°/3.3°	0.32876	354.0°/83.8°	498.02	1.012	1.015	1.027	0.063
HW7	35°	20°	9	0.33857	238.6°/0.7°	0.33805	328.7°/6.7°	0.32338	142.5°/83.2°	802.81	1.004	1.048	1.052	0.807
HW8	62°	18°	9	0.33509	42.4°/1.1°	0.33394	132.5°/4.6°	0.33097	299.1°/85.3°	359.03	1.004	1.017	1.020	0.547
HW9	58°	15°	11	0.33806	40.6°/2.2°	0.33769	131.2°/14.0°	0.32426	301.9°/75.8°	683.64	1.003	1.040	1.044	0.796
HW10	47°	12°	9	0.33567	45.5°/6.7°	0.33423	137.2°/13.9°	0.33010	290.3°/74.5°	223.70	1.005	1.013	1.018	0.421

N, number of specimens; τ_n, eigenvalues; τ_n T/P, Trend and plunge of eigenvectors in situ; χ_m, mean bulk susceptibility; $L = \tau_1/\tau_2$; $F = \tau_2/\tau_3$; $P = \tau_1/\tau_3$; $T = 2*(((\log(\tau_2/\tau_3))/(\log(\tau_1/\tau_3)))$.

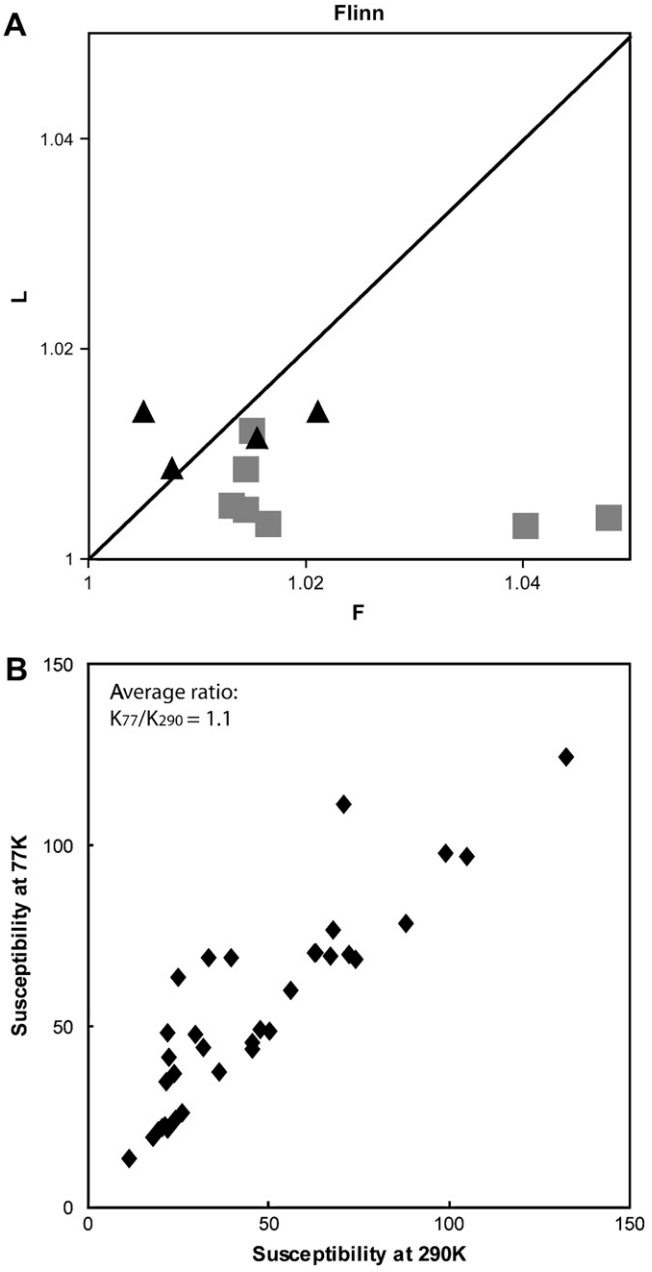

Fig. 7. (A) Flinn diagram plotting L (K_{int}/K_{max}) and F (K_{int}/K_{min}). Squares (triangles) represent hanging wall (footwall) site means. (B) Bulk susceptibility given in SI units measured at both room temperature (290K) and liquid nitrogen temperature (77K). Average ratio between the two measurements is 1.1.

calculations were performed using the GSG/Strain99 program of Evans and Groshong (1994).

5.2. Results

Calcite twinning analysis reveals compression directions that are mostly within the bedding plane and tension directions that are approximately orthogonal to the bedding plane at all sites, indicating a prefolding, layer-parallel fabric in all sites (Table 4). Calculated strain-axis orientations are similar to the Turner stress axes, ($\sigma_1 \approx e_1$, $\sigma_2 \approx e_2$, $\sigma_3 \approx e_3$). However,

Table 4
Calcite twinning results from the Ordovician Chickamauga limestones

	Latitude	Longitude	Strike	Dip	N	Std Error	% Strain	% NEV	*N* NEV	e_1	e_1 *T/P*	e_2	e_2 *T/P*	e_3	e_3 *T/P*	σ_1 *T/P*	σ_2 *T/P*	σ_3 *T/P*
Footwall																		
CFW1	33.18°N	87.23°W	274°	101°N	60	0.117	1.582	1.7	1	−1.778	195.4°/12.4°	0.525	39.8°/76.4°	1.253	286.6°/5.4°	204.1°/12.2°	73.3°/71.8°	297.0°/13.4°
CFW2	33.33°N	87.05°W	212°	76°W	82	0.137	1.385	0.0	0	−1.533	98.1°/17.8°	0.372	1.6°/19.6°	1.161	227.2°/63.1°	100.0°/14.3°	349.7°/53.7°	199.4°/32.5°
CFW3	33.71°N	86.62°W	193°	4°W	92	0.052	0.615	2.2	2	−0.702	291.8°/1.3°	0.26	21.8°/2.0°	0.442	169.8°/87.6°	292.0°/2.7°	22.4°/8.1°	183.4°/81.5°
CFW4	33.73°N	86.62°W	290°	3°N	134	0.131	1.526	0.0	0	−1.496	96.4°/11.3°	−0.058	278.1°/78.7°	1.554	186.5°/0.3°	96.6°/14.2°	252.3°/74.5°	5.1°/6.1°
Hangingwall																		
CHW1	33.45°N	86.87°W	58°	25°SE	87	0.095	0.987	1.1	1	−0.989	310.7°/12.1°	0.004	218.5°/10.2°	0.985	89.6°/74.1°	307.5°/13.0°	38.0°/2.0°	136.6°/76.8°
CHW2	33.50°N	86.79°W	55°	19°SE	83	0.043	0.828	2.4	2	−0.874	307.0°/5.5°	0.102	216.4°/6.0°	0.772	78.8°/81.8°	309.3°/3.0°	39.5°/4.8°	186.8°/84.3°
CHW3	33.53°N	86.73°W	60°	24°SE	105	0.034	0.595	1.9	2	−0.640	319.0°/6.1°	0.103	228.8°/1.6°	0.536	123.7°/83.7°	309.8°/5.9°	41.2°/12.9°	195.9°/75.8°
CHW4	33.55°N	86.71°W	41°	12°SE	84	0.037	0.404	6.0	5	−0.354	171.7°/7.8°	−0.086	81.3°/2.7°	0.44	332.4°/81.7°	180.6°/6.4°	270.7°/0.4°	4.2°/83.6°

N, number of twinsets; Std Error, nominal error; % Strain, total strain; % NEV, percent negative expected values; *N* NEV, number of negative expected values; e_n, maximum (e_1), medium (e_2) and minimum (e_3) strains; e_n *T/P*, orientation of strain axes; σ_n *T/P*, orientation of stress axes.

the layer-parallel σ_1 orientations show significant variation between sites (Table 4). Due to the limited number of sample sites and the fact that sample sites could not be selected due to exposure to be paired across the thrust for calcite twinning analysis, a systematic correlation between footwall and hanging wall results could not be determined (Table 4). Therefore, our hypothesis testing is primarily based on the paleomagnetic and magnetic susceptibility data.

6. Discussion

Our combined results from the analyses of samples in the hanging wall and the footwall of the Jones Valley thrust sheet are used to determine the presence and amount, if any, of rotation on the thrust front. To augment our paleomagnetic data, we include prior results from Hodych et al. (1985), who sampled the northeastern portion of the Birmingham anticlinorium (northeast of site HW8; Fig. 1B). Included from Hodych et al. (1985) are three results from the footwall and seven results from the hanging wall, although five of these hanging wall sites are near site HW8. When comparing the tilt corrected directions (Fig. 8), no discernable difference in declination is seen between hanging wall rocks and footwall rocks. A comparison of the mean directions for the footwall ($D = 147.3°$, $I = 21.4°$, $\alpha95 = 6.1°$, $k = 97.96$) and hanging wall ($D = 151.4\ °$, $I = 17.4°$, $\alpha95 = 3.0°$, $k = 181.98$) also shows that lack of declination difference (Fig. 8). Perroud and Van der Voo (1984) obtained results from the entire thrust belt in Alabama and therefore offer an independent average direction for the Red Mountain Formation. Comparison of our directions with their result ($D = 150.0°$, $I = 20.0°$, $\alpha95 = 3.5°$, $k = 64$) also shows no statistical difference (Fig. 8). Thus, paleomagnetism of the Red Mountain Formation reveals no significant vertical-axis rotation of the hanging wall of the Jones Valley thrust sheet.

Layer-parallel magnetic fabrics provide a similar result for a test of vertical-axis rotations of the Jones Valley thrust sheet. The mean trend for the K_{max} for the footwall is approximately 37° and for the hanging wall 40°, both of which are approximately parallel to the thrust trace. The generally thrust-parallel trend of K_{max} and the lack of deviation between the footwall and hanging wall layer-parallel magnetic lineations support the conclusion that no relative rotation occurred after acquisition of the fabric. Strain and AMS ellipsoids are inherently difficult to compare for a variety of reasons (see Borradaile and Henry, 1997; Pares and van der Pluijm, 2002a; Evans et al., 2003). However, in the footwall, the greater intensity of the tectonic lineation is indicative of larger strains (Fig. 7a). In the hanging wall, many sites are dominated by a compaction fabric, but tectonic lineations appear to be better developed to the southwest, where we predict more strain within the thrust sheet on the basis of cross-section restoration.

Rotation of the Jones Valley thrust fault is not supported by paleomagnetism or magnetic fabrics. Rotation, therefore, cannot explain the displacement gradient despite the geometrically measured 15°–23° apparent rotation of the thrust sheet. Therefore, instead of a rotating thrust sheet with a fixed hinge, we propose that the thrust developed by self-similar growth, with displacement perpendicular to the strike of the ramp and lateral growth of the fault coincident with increased displacement into the foreland (Fig. 9). The proposed scenario envisions growth of the thrust sheet with straight, parallel displacement vectors into the foreland, while the surface expression of the fault grows laterally in both directions. Our favored model assumes that some deformation must be accommodated within the thrust sheet to maintain continuity without tear faults, which may be accomplished by cataclastic flow within the thrust sheet (Wilkerson, 1992; Ismat and Mitra, 2005).

Our model also has implications for the thrust belt structure beneath the coastal plain cover. Displacement on the Jones Valley thrust sheet should continue to decrease southwest of cross-section 18. Therefore, to the southwest, we might expect a footwall splay to appear in a similar position as the Opossum Valley thrust fault in the northeast. This prediction would allow for further transfer of displacement from the Jones Valley thrust fault. New work to the southwest beneath the Coastal Plain cover would be useful to fully understand this relationship.

Several studies have documented displacement-length relationships on faults and determined a power-law relationship, $D_{max} = cL_{max}^{n}$, where D_{max} is the maximum displacement, L_{max} is the maximum fault length and c and n are constants (e.g., Davis et al., 2005). The half-length/displacement

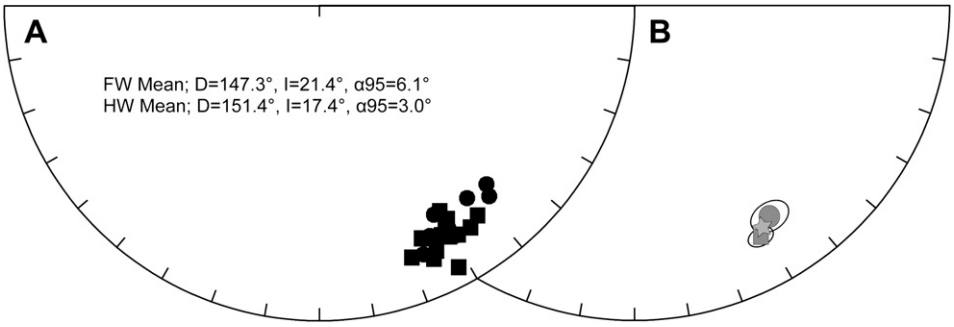

Fig. 8. (A) Lower hemisphere, equal area projections showing tilt corrected site means including data from Hodych et al. (1985). Squares (circles) represent hanging wall (footwall) sites. (B) Comparison of footwall (circle) and hanging wall (square) mean directions and associated $\alpha95$'s. Star represents mean direction of Perroud and Van der Voo (1984).

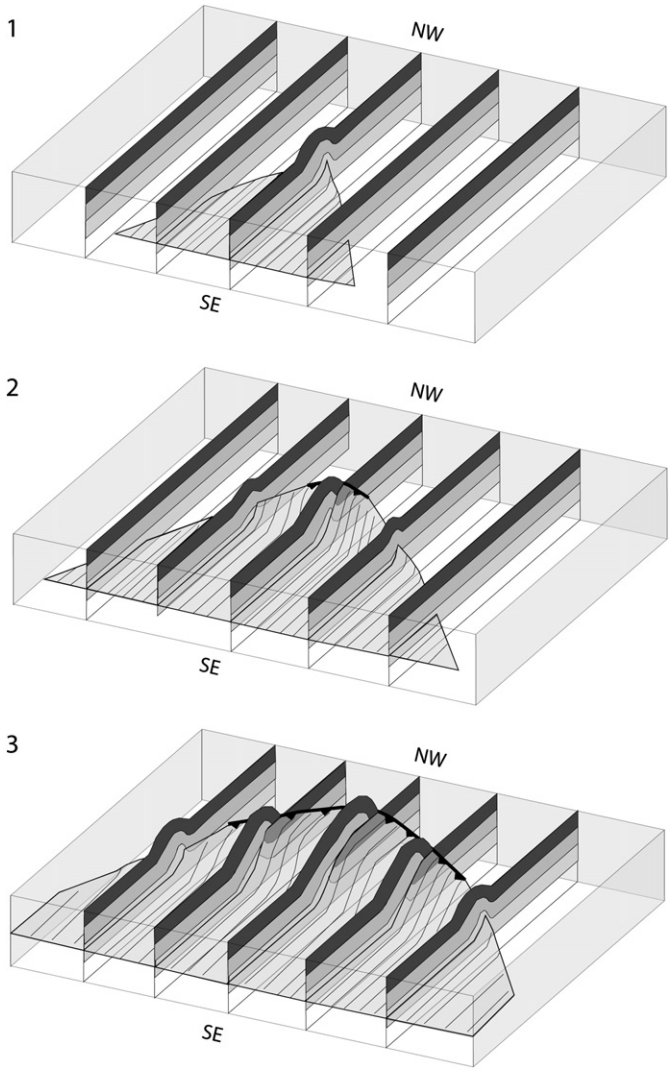

Fig. 9. Three steps in the development of a self-similar thrusting model. Transport toward the foreland occurs within the detachment fold, followed by progressive breaking of the fold and lateral growth of the thrust surface. The bulk of the transported fold has been eroded away in the Jones Valley thrust sheet.

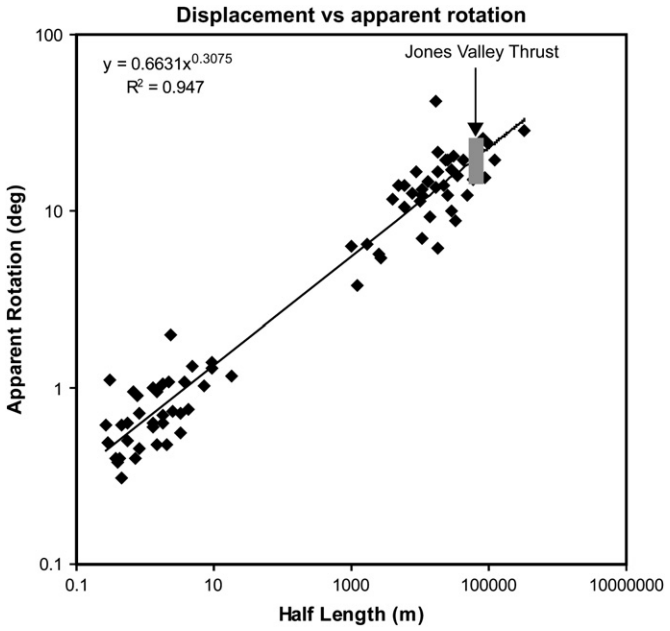

Fig. 10. Plot of the relationship between fault half-length and the apparent rotation. The range of apparent rotations angles for the Jones Valley thrust lies within the scale of many thrusts. Data taken from Davis et al. (2005) and Hatcher (2004).

relationships of thrust faults from Davis et al. (2005) and Hatcher (2004) were compiled and converted into apparent rotation vs. displacement to evaluate whether the Jones Valley thrust fault has a similar relationship between calculated rotation and half-length (Fig. 10). The range of apparent rotation angles (15°–23°) for the Jones Valley thrust fault is consistent with other thrust faults. Therefore, the proposed displacement gradient is comparable to other non-rotated thrust sheets.

7. Conclusion

Paleomagnetism of the Red Mountain Formation reveals a prefolding magnetization, likely acquired in the Pennsylvanian, prior to motion on the Jones Valley thrust fault. The displacement gradient on the Jones Valley thrust fault produced 15°–23° of curvature. However, paleomagnetic directions and magnetic fabric K_{max} orientations reveal no discernable difference between the hanging wall and the footwall of the Jones Valley thrust sheet. Thus, vertical-axis rotation of the hanging wall does not explain the observed displacement gradient. Instead, using a self-similar model of thrusting, we argue that the Jones Valley thrust sheet grew laterally as it progressed into the foreland and created a displacement gradient without significant rotation. Accommodating strain is proposed to have accumulated within the thrust sheet as it developed via cataclastic flow. This work shows that displacement gradients do not need to be associated with vertical-axis rotations. Also, caution is advised when interpreting rotations in foreland thrust belts based purely on kinematic modeling without independent data, such as paleomagnetism or other passive structural markers.

Acknowledgements

Appalachian research at the University of Michigan was supported by grants from the American Chemical Society-Petroleum Research Fund (most recently 45893-AC8), by the Scott Turner Fund and student grants from the Geological Society of America. We thank Franek Hasiuk and Ed Osborne for field support, Josep Parés for laboratory support and Rick Allmendinger for his Stereonet program. The authors would also like to thank journal reviewers David Wiltschko and Emilio Pueyo for thorough and thoughtful reviews that significantly improved the manuscript.

References

Allerton, S., 1994. Vertical-axis rotation associated with folding and thrusting; an example from the eastern Subbetic Zone of southern Spain. Geology 22, 1039–1042.

Allerton, S., 1998. Geometry and kinematics of vertical axis rotations in fold and thrust belts. Tectonophysics 299, 15–30.

Allerton, S., Lonergan, L., Platt, J.P., Platzman, E.S., McClelland, E., 1993. Palaeomagnetic rotations in the eastern Betic Cordillera, southern Spain. Earth and Planetary Science Letters 119, 225–241.

Apotria, T.G., 1995. Thrust sheet rotation and out-of-plane strains associated with oblique ramps: an example from the Wyoming salient. U.S.A. Journal of Structural Geology 17, 647–662.

Bates, M.P., 1989. Palaeomagnetic evidence for rotations and deformation in the Nogueras Zone, Central Southern Pyrenees, Spain. Journal of the Geological Society of London 146, 459–476.

Bayona, G., Thomas, W.A., Van der Voo, R., 2003. Kinematics of thrust sheets within transverse zones: a structural and paleomagnetic investigation in the Appalachian thrust belt of Georgia and Alabama. Journal of Structural Geology 25, 1193–1212.

Berdan, J.M., Boucot, A.J., Ferrill, B.A., 1986. The first fossiliferous Pridolian beds from the Southern Appalachians in northern Alabama, and the age of the uppermost Red Mountain Formation. Journal of Paleontology 60, 180–185.

Berry, W.B.N., Boucot, A.J. (Eds.), 1970. Correlation of the North American Silurian rocks. Geological Society of America Special Paper, 102, p. 289.

Borradaile, G., Henry, B., 1997. Tectonic applications of magnetic susceptibility and its anisotropy. Earth-Science Reviews 42, 49–93.

Butts, 1926 Butts, C., 1926, The Paleozoic rocks *in* Geology of Alabama: Alabama Geological Survey Special Report 14, 41–230.

Chowns, T.M., McKinney, F.K., 1980. Depositional facies in Middle-Upper Ordovician and Silurian rocks of Alabama and Georgia. In: Frey, R.W. (Ed.), Excursions in Southeastern Geology. Geological Society of America Annual Meeting Field Trip Guide, Atlanta, Georgia, Volume II. American Geological Institute, Falls Church, Virginia, pp. 323–348.

Cifelli, F., Rossetti, F., Mattei, M., Hirt, A.M., Funiciello, R., Tortorici, L., 2004. An AMS, structural and paleomagnetic study of Quaternary deformation in eastern Sicily. Journal of Structural Geology 26, 29–46.

Craddock, J.P., Kopania, A.A., Wiltschko, D.V., 1988. Interaction between the northern Idaho-Wyoming thrust belt and bounding basement blocks, central western Wyoming. Geological Society of America Memoir 171, 333–351.

Dahlstrom, C.D.A., 1969. Balanced cross sections. Canadian Journal of Earth Sciences 6, 743–757.

Davis, K., Burbank, D.W., Fisher, D., Wallace, S., Nobes, D., 2005. Thrust-*fault* growth and segment linkage in the active Ostler *fault* zone, New Zealand. Journal of Structural Geology 27, 1528–1546.

Elliott, D., 1976. The energy balance and deformation mechanisms of thrust sheets. Philosophical Transactions of the Royal Society of London A283, 289–312.

Engelder, T., 1979. The nature of deformation within the outer limits of the central Appalachian foreland fold and thrust belt in New York State. Tectonophysics 55, 289–310.

Evans, M.A., Groshong, R.H., 1994. A computer program for the calcite strain-gauge technique. Journal of Structural Geology 16, 277–282.

Evans, M.A., Lewchuk, M.T., Elmore, R.D., 2003. Strain partitioning of deformation mechanisms in limestones; examining the relationship of strain and *anisotropy* of magnetic susceptibility (AMS). Journal of Structural Geology 25, 1525–1549.

Fisher, R.A., 1953. Dispersion on a sphere. Proceedings of the Royal Society of London A 217, 295–305.

Fischer, M.P., Woodward, N.B., 1992. The geometric evolution of foreland thrust systems. In: McClay, K.R. (Ed.), Thrust Tectonics. Chapman & Hall, London, United Kingdom.

Gray, M.B., Mitra, G., 1993. Migration of deformation fronts during progressive deformation: evidence from detailed structural studies in the Pennsylvania Anthracite region, U.S.A. Journal of Structural Geology 15, 435–449.

Groshong, R.H., 1972. Strain calculated from twinning in calcite. Geological Society of America Bulletin 83, 2025–2038.

Groshong, R.H., 1974. Experimental test of least-squares strain gage calculation using twinned calcite. Geological Society of America 85, 1855–1864.

Groshong, R.H., Teufel, L.W., Gasteiger, C., 1984. Precision and accuracy of the calcite strain-gauge technique. Geological Society of America 95, 357–363.

Hatcher Jr., R.D., 2004. Properties of thrusts and upper bounds for the size of thrust sheets. AAPG Memoir 82, 18–29.

Hatcher Jr., R.D., Thomas, W.A., Geiser, P.A., Snoke, A.W., Mosher, S., Wiltschko, D.V., 1989. Alleghanian orogeny. In: Hatcher Jr., R.D., Thomas Jr., W.A., Viele, G.W. (Eds.), The Appalachian-Ouachita Orogen in the United StatesThe Geology of North America (Decade of North American Geology, F-2). Geological Society of America, Boulder, CO, pp. 233–318.

Hodych, J.P., Paetzold, R.R., Buchan, K.L., 1985. Chemical remanent magnetization due to deep-burial diagenesis in oolitic hematite-bearing ironstones of Alabama. Physics of the Earth and Planetary Interiors 37, 261–284.

House, W.M., Gray, D.R., 1982. Cataclasites along the Saltville thrust, USA and their implications for thrust sheet emplacement. Journal of Structural Geology 4, 257–269.

Ismat, Z., Mitra, G., 2005. Fold-thrust belt evolution expressed in an internal thrust sheet, Sevier Orogen; the role of cataclastic flow. Geological Society of America Bulletin 117, 764–782.

Jelinek, V., 1978. Statistical processing of anisotropy of magnetic susceptibility measured on groups of specimens. Studia Geophysica et Geodetica 22, 50–62.

Kirschvink, J.L., 1980. The least-square line and plane and the analysis of palaeomagnetic data. Geophysical Journal of the Royal Astronomical Society 62, 699–718.

Kollmeier, J.M., van der Pluijm, B.A., Van der Voo, R., 2000. Analysis of Variscan dynamics; early bending of the Cantabria-Asturias Arc, northern Spain. Earth and Planetary Science Letters 181, 203–216.

Macedo, J., Marshak, S., 1999. Controls on the geometry of fold-thrust belt salients. Geological Society of America Bulletin 111, 1808–1822.

Marshak, S., 2004. Salients, recesses, arcs, oroclines, and syntaxes—a review of ideas concerning the formation of map-view curves in fold-thrust belts. In: McClay, K.R. (Ed.), Thrust Tectonics and Hydrocarbon Systems: AAPG Memoir 82, pp. 1–26.

Marshak, S., Mitra, G., 1988. Basic Methods of Structural Geology. Prentice Hall, New Jersey, 446 p.

McCaig, A.M., McClelland, E., 1992. Paleaeomagnetic techniques applied to thrust belts. In: McClay, K.R. (Ed.), Thrust Tectonics: New York. Chapman and Hall, New York, pp. 209–216.

McElhinny, M.W., 1964. Statistical significance of the fold test in paleomagnetism. Geophysical Journal of the Royal Astronomical Society 8, 338–340.

Nickelsen, R.P., 1979. Sequence of structural stages of the Alleghany orogeny, Bear Valley strip mine, Shamokin, PA. American Journal of Science 279, 225–271.

O'Hara, K., Kanda, R., Thomas, W.A., 2006. Thermal footprint of an eroded thrust sheet in the southern Appalachian Black Warrior basin, Alabama. Geological Society of America Abstracts with Programs 38 no. 3, 7.

Oliva-Urcia, B., Pueyo, E.L., 2007. Gradient of shortening and vertical-axis rotations in the Southern Pyrenees (Spain), insights from a synthesis of paleomagnetic data. Revista de la Sociedad Geológica de España.

Ong, P.F., Pluijm, B.A., Van der Voo, R., 2007. Early rotation in the Pennsylvania Salient (US Appalachians): evidence from calcite-twinning analysis of Paleozoic carbonates. Geological Society of America Bulletin 119, 796–804.

Pares, J.M., van der Pluijm, B.A., 2002a. Evaluating magnetic lineations (AMS) in deformed rocks. Tectonophysics 350, 283–298.

Pares, J.M., van der Pluijm, B.A., 2002b. Phyllosilicate fabric characterization by Low-Temperature Magnetic Anisotropy (LT-AMS). Geophysical Research Letters, doi:10.1029/2002GL015459.

Perroud, H., Van der Voo, R., 1984. Secondary magnetizations from the Clinton-type iron ores of the Silurian Red Mountain Formation, Alabama. Earth and Planetary Science Letters 67, 391–399.

Pueyo, E.L., Millán, H., Pocovi, A., 2002. Rotation velocity of a thrust; a paleomagnetic study in the External Sierras (southern Pyrenees). Sedimentary Geology 146, 191–208.

Pueyo, E.L., Pocovi, A., Millán, H., Sussman, A.J., 2004. Map-view models for correcting and calculating shortening estimates in rotated thrust fronts

using paleomagnetic data. Geological Society of America Special Paper 383, 57–71.

Richter, C., van der Pluijm, B.A., 1994. Separation of paramagnetic and ferrimagnetic susceptibilities using low temperature magnetic susceptibilities and comparison with high field methods. Physics of the Earth and Planetary Interiors 82, 113–123.

Rindsberg, A.K., Osborne, W.E., 2001. Geology of the Bessemer 7.5 minute quadrangle, Jefferson County, Alabama. Alabama Geological Survey Quadrangle Series 20, 25, p, 2 pl.

Rindsberg, A.K., Ward, W.E., Osborne, W.E., Irvin, G.D., 2003. Geology of the Irondale 7.5 minute quadrangle, Jefferson County, Alabama. Alabama Geological Survey Quadrangle Series 26, 36, p, 2 pl.

Rodgers, J., 1970. The Tectonics of the Appalachians. Wiley Interscience, New York, 271 p.

Saint-Bezar, B., Hebert, R.L., Aubourg, C., Robion, P., Swennen, R., Frizon de Lamotte, D., 2002. Magnetic fabric and petrographic investigation of hematite-bearing sandstones within ramp-related folds; examples from the South Atlas Front (Morocco). Journal of Structural Geology 24, 1507–1520.

Satolli, S., Speranza, F., Calamita, F., 2005. Paleomagnetism of the Gran Sasso range salient (central Apennines, Italy): pattern of orogenic rotations due to translation of a massive carbonate indenter. Tectonics 24, TC4019.

Schwartz, S.Y., Van der Voo, R., 1984. Paleomagnetic study of thrust sheet rotation during foreland impingement in the Wyoming-Idaho overthrust belt. Journal of Geophysical Research 89, 10077–10086.

Somma, R., 2006. The south-western side of the Calabrian Arc (Peloritani Mountains): geological, structural and AMS evidence for passive clockwise rotations. Journal of Geodynamics 41, 422–439.

Soto, R., Casas-Sainz, A.M., Pueyo, E.L., 2006. Along-strike variation of orogenic wedges associated with vertical axis rotations. Journal of Geophysical Research 111, B10402.

Spang, J.H., 1972. Numerical method for dynamic analysis of calcite twin lamellae. Geological Society of America Bulletin 83, 467–472.

Spang, J.H., Groshong, R.H., 1981. Deformation mechanisms and strain history of a minor fold from the Appalachian Valley and Ridge Province. Tectonophysics 72, 323–342.

Speranza, F., Adamoli, L., Maniscalco, R., Florindo, F., 2003. Genesis and evolution of a curved mountain front; paleomagnetic and geological evidence from the Gran Sasso Range (Central Apennines, Italy). Tectonophysics 362, 183–197.

Sussman, A.J., Butler, R.F., Dinares-Turell, J., Verges, J., 2004. Vertical-axis rotation of a foreland fold and implications for orogenic curvature: an example from the Southern Pyrenees, Spain. Earth and Planetary Science Letters 218, 435–449.

Szabo, M.W., Osborne, E.W., Copeland, C.W., 1988. Geologic Map of Alabama, Northewest Sheet. Alabama Geological Survey Special Map 220 scale 1:250,000.

Tauxe, L., 1998. Paleomagnetic Principles and Practice: Boston. Kluwer Academic Publishers, 299 pp.

Teufel, L.W., 1980. Strain analysis of experimental superposed deformation using calcite twin lamellae. Tectonophysics 65, 291–309.

Thomas, W.A., 1977. Evolution of Appalachian-Ouachita salients and recesses from reentrants and promontories in the continental margin. American Journal of Science 277, 1233–1278.

Thomas, W.A., 1991. The Appalachian-Ouachita rifted margin of southeastern North America. Geological Society of America Bulletin 103, 415–431.

Thomas, W.A., 2001. Mushwad: ductile duplex in the Appalachian thrust belt in Alabama. American Association of Petroleum Geologists Bulletin 85, 1847–1869.

Thomas, W.A., Bayona, G., 2002. Palinspastic restoration of the Anniston Transverse Zone in the Appalachian thrust belt, Alabama. Journal of Structural Geology 24, 797–826.

Thomas, W.A., Bayona, G., 2005. The Appalachian thrust belt in Alabama and Georgia: thrust-belt structure, basement structure, and palinspastic reconstruction. Geological Survey of Alabama Monograph 16, 48.

Thomas, W.A., Bearce, D.N., 1986. Birmingham Anticlinorium in the Appalachian fold-thrust belt, basement fault system, synsedimentary structure, and thrust ramp. In: Neathery, T.L. (Ed.), Centennial Field Guide Volume 6, Southeastern Section of the Geological Society of America. Geological Society of America, Boulder Colorado, pp. 191–200.

Torsvik, T., Briden, J.C., Smethurst, M.A., 1999. SuperIAPD1999 – Software Package. Geological Survey of Norway, Trondheim.

Tull, J.F., 1998. Analysis of a regional middle Paleozoic unconformity along the distal southeastern Laurentian margin, southernmost Appalachians: implications for tectonic evolution. Geological Society of America Bulletin 110, 1149–1162.

Turner, F.J., 1953. Nature and dynamic interpretation of deformation lamellae in calcite of three marbles. American Journal of Science 251, 276–298.

Van der Voo, R., 1993. Paleomagnetism of the Atlantic. Tethys and Iapetus Oceans. Cambridge University Press, New York, NY, 411 pp.

Weil, A.B., Sussman, A., 2004. Classification of curved orogens based on the timing relationships between structural development and vertical-axis rotations, in: paleomagnetic and structural analysis of orogenic curvature. Geologic Society of America Special Paper 383, 1–17.

Weil, A.B., Van der Voo, R., van der Pluijm, B.A., Pares, J., 2000. The formation of an orocline by multiphase deformation; a paleomagnetic investigation of the Cantabria Asturias Arc (northern Spain). Journal of Structural Geology 22, 735–756.

Weil, A.B., Van der Voo, R., van der Pluijm, B., 2001. New paleomagnetic data from the southern Cantabria-Asturias Arc, northern Spain: implications for true oroclinal rotation and the final amalgamation of Pangea. Geology 29, 991–994.

Wilkerson, M.S., 1992. Differential transport and continuity of thrust sheets. Journal of Structural Geology 14, 749–751.

Winston, R.B., 1990. Vitrinite reflectance of Alabama's bituminous coal. Alabama Geological Survey Circular 139, 54.

Zijderveld, J.D.A., 1967. AC demagnetization of rocks: analysis of results. In: Collinson, D.W., Creer, K.M. (Eds.), Methods in Paleomagnetism. Elsevier, Amsterdam, pp. 254–286.